

SPECIAL TOPIC

# MoS<sub>2</sub> saturable absorber prepared by chemical vapor deposition method for nonlinear control in Q-switching fiber laser

To cite this article: Meng-Li Liu *et al* 2018 *Chinese Phys. B* **27** 084211

View the [article online](#) for updates and enhancements.

## Related content

- [Large-area and highly crystalline MoSe<sub>2</sub> for optical modulator](#)  
Jinde Yin, Hao Chen, Wei Lu *et al.*
- [CVD-grown MoSe<sub>2</sub> with high modulation depth for ultrafast mode-locked erbium-doped fiber laser](#)  
Wenjun Liu, Mengli Liu, Yuyi OuYang *et al.*
- [Tungsten diselenide for mode-locked erbium-doped fiber lasers with short pulse duration](#)  
Wenjun Liu, Mengli Liu, Yuyi OuYang *et al.*

# MoS<sub>2</sub> saturable absorber prepared by chemical vapor deposition method for nonlinear control in Q-switching fiber laser \*

Meng-Li Liu(刘孟丽)<sup>1</sup>, Yu-Yi OuYang(欧阳毓一)<sup>1</sup>, Huan-Ran Hou(侯焕然)<sup>1</sup>,  
Ming Lei(雷鸣)<sup>1</sup>, Wen-Jun Liu(刘文军)<sup>1,2,†</sup>, and Zhi-Yi Wei(魏志义)<sup>2,‡</sup>

<sup>1</sup>State Key Laboratory of Information Photonics and Optical Communications, School of Science,  
Beijing University of Posts and Telecommunications, Beijing 100876, China

<sup>2</sup>Beijing National Laboratory for Condensed Matter Physics, Institute of Physics,  
Chinese Academy of Sciences, Beijing 100190, China

(Received 25 April 2018; revised manuscript received 20 May 2018; published online 10 July 2018)

Due to the remarkable carrier mobility and nonlinear characteristic, MoS<sub>2</sub> is considered to be a powerful competitor as an effective optical modulated material in fiber lasers. In this paper, the MoS<sub>2</sub> films are prepared by the chemical vapor deposition method to guarantee the high quality of the crystal lattice and uniform thickness. The transfer of the films to microfiber and the operation of gold plated films ensure there is no heat-resistant damage and anti-oxidation. The modulation depth of the prepared integrated microfiber-MoS<sub>2</sub> saturable absorber is 11.07%. When the microfiber-MoS<sub>2</sub> saturable absorber is used as a light modulator in the Q-switching fiber laser, the stable pulse train with a pulse duration of 888 ns at 1530.9 nm is obtained. The ultimate output power and pulse energy of output pulses are 18.8 mW and 88 nJ, respectively. The signal-to-noise ratio up to 60 dB indicates the good stability of the laser. This work demonstrates that the MoS<sub>2</sub> saturable absorber prepared by the chemical vapor deposition method can serve as an effective nonlinear control device for the Q-switching fiber laser.

**Keywords:** nonlinear optical materials, fiber laser, Q-switching

**PACS:** 42.70.Mp, 42.55.Wd, 42.60.Gd

**DOI:** 10.1088/1674-1056/27/8/084211

## 1. Introduction

The saturable absorber (SA), as a natural light modulation device, is the key part of the pulsed fiber laser in Q-switching and mode-locking. Semiconductor saturable absorber mirrors (SESAMs) are the most well-researched and mature SAs, and we attribute the success in application to the controllable absorption wavelength, saturation threshold, modulation depth, and relaxation time.<sup>[1,2]</sup> However, the relatively high cost and narrow working bandwidth of SESAM have urged researchers to seek new alternatives for them. Then, the rise of graphene has meant two-dimensional (2D) materials are gradually being used more and more.<sup>[3]</sup> Some of the most representative materials that can be used as SAs have been studied in depth.<sup>[4,5]</sup> The unique zero band gap structure of graphene impels it to own the wider working wavelength than other 2D materials. The ultrafast recovery time and strong nonlinearity of graphene further prove that graphene can be a powerful candidate for SA.<sup>[6–9]</sup> Topological insulators (TIs) are also interesting because of their large modulation depth and nonlinearity.<sup>[10–13]</sup> The superiorities of TIs in light modulation contribute to their great potential in optoelectronics applications. Black phosphorus (BPs) maintain a direct band gap

whether they are a bulk or layered structure. Their band gap is adjustable from 0.3 eV to 1.5 eV, which indicates that it is easy to make a breakthrough in the application of photon and photoelectron in the near infrared band.<sup>[14–18]</sup> In addition to these classic materials, some novel 2D materials have also begun to arouse interest due to their unique electronic and optical characteristics. BP quantum dots (BPQDs), which are able to combine the quantum confinement and edge effects, exhibit excellent nonlinear optical response according to previous studies.<sup>[19]</sup> Moreover, BPQDs have been successfully used in mode-locked erbium-doped fiber laser (EDFL). MXene, as another kind of new member of the 2D material family, shows good conductivity, tunable bandgap, and ability to perform ion intercalation. It has reported that MXene performs optical manipulation in photonic applications, similar to or better than graphene.<sup>[20]</sup>

In transition metal dichalcogenides (TMDs), a layer of *M* (Mo, W, etc.) atoms is sandwiched between two layers of *X* (S, Se, etc.) atoms, so the chemical formula of TMDs is generally written as *MX*<sub>2</sub>. The neighbor layers of TMDs are bonded with weak van der Waals force, which indicates layered nanosheets are easily separated from the sample.<sup>[21–36]</sup> From previous work, the band gap of TMD varies with the number of lay-

\*Project supported by the National Natural Science Foundation of China (Grant No. 11674036), the Beijing Youth Top-notch Talent Support Program, China (Grant No. 2017000026833ZK08), the Fund of State Key Laboratory of Information Photonics and Optical Communications, Beijing University of Posts and Telecommunications, China (Grant Nos. IPOC2016ZT04 and IPOC2017ZZ05).

†Corresponding author. E-mail: jungliu@bupt.edu.cn

‡Corresponding author. E-mail: zywei@iphy.ac.cn

ers, and so the consequent layer-dependent electronic and optical characteristics are attracting increasing attention.<sup>[37–39]</sup> Among TMDs, MoS<sub>2</sub> is prominent considering its performance in photoelectrons. It is reported that the nonlinear optical response of MoS<sub>2</sub> is better than graphene.<sup>[40,41]</sup> The few-layer MoS<sub>2</sub> unambiguously exhibits broadband absorption from previous work.<sup>[42]</sup> Furthermore, it is found that the starting Q-switching operation threshold of MoS<sub>2</sub> is small under the same experimental conditions compared with those of the materials of the same kind.<sup>[43]</sup> The relaxation time of MoS<sub>2</sub> is estimated at  $\sim 30$  fs as mentioned in Ref. [44], which indicates that it has potential for fabricating the ultra-fast electronic devices.

There are various methods to be chosen in the fabrication of SA. The two most representative top-down methods are mechanical exfoliation (ME)<sup>[45,46]</sup> with the aid of scotch tapes, and liquid-phase exfoliation (LPE)<sup>[47,48]</sup> getting dispersant through ultrasonication and centrifugation. These two methods are convenient and low-cost, but the layer number of prepared nanosheets is random. By comparison, the three bottom-up methods, as the common methods, have better performance in the control of the layer number and the quality of the sample, they are the pulsed laser deposition (PLD) method,<sup>[49,50]</sup> chemical vapor deposition (CVD) method,<sup>[51,52]</sup> and magnetron sputtering deposition (MSD) method,<sup>[53,54]</sup> respectively. From previous reports, the layer number of nanosheets prepared by the CVD method tends to be controlled more accurately through adjusting the reaction parameters.

Here in this paper, the MoS<sub>2</sub> produced through the CVD method is moved to the waist of the microfiber to form MoS<sub>2</sub> SA. Finally, the effective area of the taper fiber is fully covered with gold to prevent it from being oxidized. By means of the interaction between the evanescent field of light and the material, the SA is able to avoid some thermal damage.<sup>[55]</sup> Furthermore, the long reaction length promotes the MoS<sub>2</sub> SA to fully exhibit the optical nonlinearity. The modulation depth (MD) and saturable intensity of MoS<sub>2</sub> SA are measured to be 11.07% and 1.871 MW/cm<sup>2</sup>, respectively. The proposed MoS<sub>2</sub> based Q-switching EDFL operates at 1530.9 nm. The corresponding pulse duration and maximum output power are 888 ns and 18.8 mW, respectively. The signal-to-noise ratio (SNR) (up to 60 dB) indicates the stability of the laser. The experimental results further prove the favorable optical modulation ability of MoS<sub>2</sub> SA.

## 2. Preparation and characterization of MoS<sub>2</sub> SA

The MoS<sub>2</sub> nanosheets were grown on the ultrathin quartz plate by the CVD method. Before the synthesis, the sulfur powder of 0.5 g was placed in the reaction chamber, and the MoO<sub>3</sub> powder of 0.5 g was placed in the heating center, which was at the downstream of sulfur powder. The ultrathin

quartz plate was placed at the downstream of the heating center, which was 20 cm away from MoO<sub>3</sub> powder. During the synthesis, the pressure of the chamber was set to be 0.1 Torr (1 Torr =  $1.33322 \times 10^2$  Pa). Under the drive of Ar flow gas, MoO<sub>3</sub> and sulfur vapors were capable of mixing and reacting fully, as the product was brought to the substrate. Because temperature is a key factor for determining the quality of the finished product, the temperature of the chamber was rising at a constant speed of 25 °C/min. The reaction chamber was heated up to 550 °C and maintained this temperature for 0.5 h, then the reaction was finished.

When the chamber cooled down to room temperature, ultrathin quartz plate attached with MoS<sub>2</sub> film was achieved. To prevent the lattice structure of MoS<sub>2</sub> film from destructing during transfer, the polymethyl methacrylate (PMMA) assisted method was adopted. Before the transfer, the PMMA was spin coated on a large scale over the MoS<sub>2</sub> film. The MoS<sub>2</sub> PMMA was able to be easily separated from ultrathin quartz plate after the open-air drying of the sample. To obtain the pure MoS<sub>2</sub> film, the MoS<sub>2</sub>PMMA was etched in acetone. Then the pure MoS<sub>2</sub> film was soaked in deionized water, which could not only remove the remnants, but also make the film float smoothly with the help of water tension. Finally, the MoS<sub>2</sub> film was moved to the conical area of microfiber (SMF-28e), which was observed by using a microscope. The measured diameter of the tapered waist was 12  $\mu\text{m}$ , and the effective contact length between the MoS<sub>2</sub> film and fiber was about 2 mm. After the volatilization of superfluous deionized water, the MoS<sub>2</sub> film closely adhered to the lateral wall of tapered fiber due to van der Waals interaction. Finally, the effective area of the microfiber was fully covered with gold to avoid rapidly oxidizing the material.

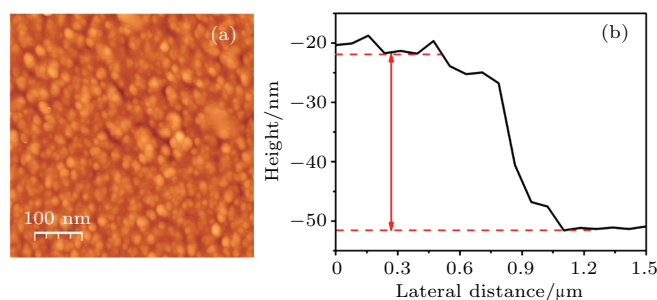


**Fig. 1.** (color online) (a) Surface morphology image of MoS<sub>2</sub> film; (b) altitude difference of the surface.

With the aid of the atomic force microscope (AFM), an important device for the nano-scale measurement, we obtained the morphology of the MoS<sub>2</sub> surface without damaging the material. Figure 1(a) shows the particles of the material are arranged closely and orderly, which indicates the MoS<sub>2</sub> films prepared by the CVD method are of great uniformity and crystallinity. The comparison of surface height among different regions on the MoS<sub>2</sub> films shows the thickness of MoS<sub>2</sub> film was 30 nm as indicated in Fig. 1(b), which corresponds to 41–42 layers in structure.

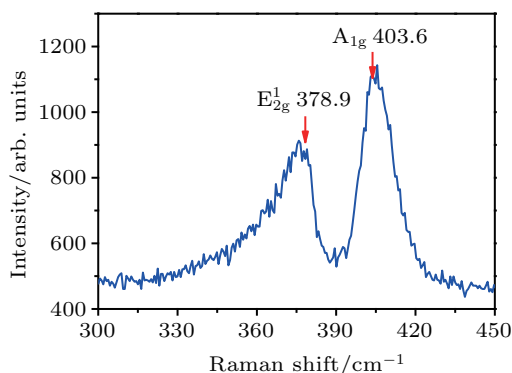


Fig. 2. (color online) Raman spectra of prepared MoS<sub>2</sub> films.

Raman spectroscopy is considered to be an effective method of determining the specific vibration modes of the material. In Fig. 2, two distinct characteristic peaks are located at 378.9 cm<sup>-1</sup> and 403.6 cm<sup>-1</sup>. According to previous research, the mode at 378.9 cm<sup>-1</sup> comes from the inplane vibration which belongs to Mo and S atoms, while the mode at 403.6 cm<sup>-1</sup> comes from the out-of-plane vibration which belongs to S atoms.<sup>[56–58]</sup> The frequency difference between two peaks illustrates the multilayer structure of prepared MoS<sub>2</sub> film.

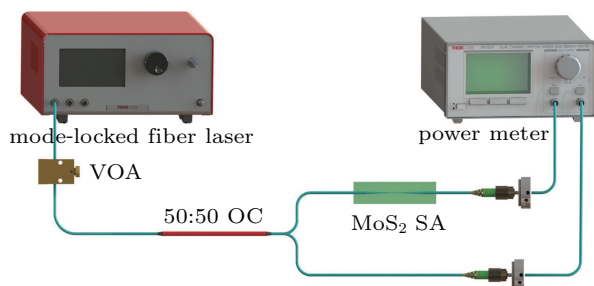


Fig. 3. (color online) Schematic diagram of power-dependent feature measurement.

The schematic diagram of power-dependent feature measurement is shown in Fig. 3. The light source was a mode-locked fiber laser operating at 1561 nm, of which the pulse duration and the repetition rate were 200 fs and 67 MHz. A variable fiber optic attenuator (VOA) was used to manually adjust

the signal attenuation when the optical signal passes through the device. By employing OC, the optical signal could be divided into two parts: one passed through MoS<sub>2</sub> SA to measure its saturated absorptive properties, and the other passed through SMF 28e for comparison. The optical signals at both ends were captured and recorded simultaneously by a power meter. Experimental data could be fitted by

$$\alpha(I) = \frac{\alpha_s}{1 + I/I_{\text{sat}}} + \alpha_{\text{ns}},$$

where  $\alpha_s$ ,  $\alpha_{\text{ns}}$ , and  $I_{\text{sat}}$  are the modulation depth, nonsaturable absorption, and saturation intensity. After the fitting of experimental data in Fig. 4, the saturable intensity and MD of MoS<sub>2</sub> SA are 1.871 MW/cm<sup>2</sup> and 11.07%, respectively.

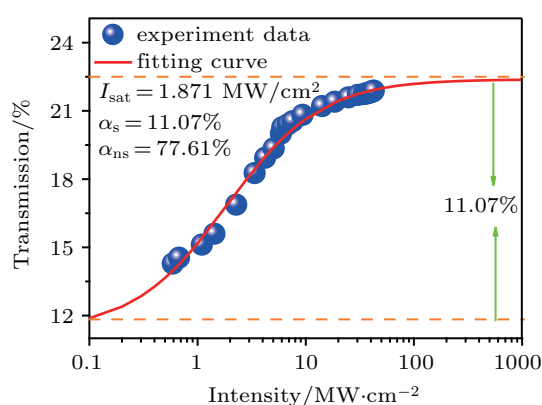


Fig. 4. (color online) Intensity-dependent transmission of MoS<sub>2</sub> SA, showing its nonlinear absorber characteristics.

In Table 1, the nonlinear parameters of MoS<sub>2</sub> SAs obtained with different fabrication methods are listed to compare the advantages of CVD-MoS<sub>2</sub>. By comparison, it can be found that CVD-MoS<sub>2</sub> generally has a large modulation depth, because the materials prepared by the CVD method have better uniformity, which is beneficial to the large modulation depth of SA. In addition, we find that the saturation intensity of CVD-MoS<sub>2</sub> is generally small, which indicates that the laser based on CVD-MoS<sub>2</sub> SA has a lower starting Q-switching operation threshold.

Table 1. Nonlinear parameters of MoS<sub>2</sub> SAs obtained with different fabrication methods.

Material	Fabrication	MD/%	Saturation intensity	Non-saturable loss/%	Ref.
MoS <sub>2</sub>	Scotch-tape micromechanical cleavage technique method	9.70	–	28.80	[59]
MoS <sub>2</sub>	Hydrothermal intercalation/exfoliation approach	10.47	–	–	[40]
MoS <sub>2</sub>	LPE	4	–	55.90	[60]
MoS <sub>2</sub>	LPE	2	10 MW/cm <sup>2</sup>	48.56	[61]
MoS <sub>2</sub>	LPE	2.15	129.4 MW/cm <sup>2</sup>	63.10	[43]
MoS <sub>2</sub>	LPE	6.30	1.6 MW/cm <sup>2</sup>	18	[62]
MoS <sub>2</sub>	LPE	1.60	13 MW/cm <sup>2</sup>	54.80	[63]
MoS <sub>2</sub>	PLD	9	27 MW/cm <sup>2</sup>	40.50	[64]
MoS <sub>2</sub>	CVD	35.40	0.34 MW/cm <sup>2</sup>	34.10	[65]
MoS <sub>2</sub>	CVD	28.50	0.55 MW/cm <sup>2</sup>	35	[66]
MoS <sub>2</sub>	CVD	11.07	1.871 MW/cm <sup>2</sup>	77.61	this work

### 3. Q-switching EDFL employed with MoS<sub>2</sub> SA

An all-fiber ring cavity in Fig. 5 was used in the experiment. Optical devices were coupled into the laser cavity in the order corresponding to the direction of propagation of light. The pump which operated at 976 nm had the maximum allowed output power of 630 mW. The 980/1550 nm WDM successfully coupled the pump light into the ring cavity for exciting the erbium-doped fiber (EDF). The group velocity dispersion (GVD) of EDF (Liekki 110-4/125) was 12 ps<sup>2</sup>/km at 1550 nm. The intra-cavity polarization and birefringence were mainly optimized by polarization controller (PC). The primary role of an isolator (ISO) is to guarantee unidirectional optical transmission in the cavity to avoid damaging the device, caused by redundant reverse light. The MoS<sub>2</sub> SA was placed between the ISO and WDM. The 20:80 optical coupler (OC) was adopted in the experiment, 20% of which was exported to monitor the real-time experimental data. The monitoring instruments used in the experiment mainly included the RF spectrum analyzer (Agilent E4402B), oscilloscope (Tektronix DPO3054), and optical spectrum analyzer (Yokogawa AQ6370C).

The stable Q-switching pulses occur at 147 mW with the increase of pump power. Meanwhile, the repetition rates of

the output pulses with different powers are recorded and exhibited in Fig. 6(a). The tunable range of frequency is 92 kHz–212 kHz. When the pump power is increased to 630 mW, the shortest pulse duration of 888 ns is obtained as shown in Fig. 6(b). The accomplished Q-switching EDFL operates at 1530.9 nm, the corresponding spectral width is 3.14 nm. For a few-hours laser operation, the time-section data of the spectrum is shown in Fig. 6(c). The almost invariable spectral shape indicates the stability of the laser. The RF spectrum of Q-switching EDFL is provided in Fig. 6(d). The SNR of the fundamental frequency increases up to 60 dB, which indicates that the operative condition of the laser is relatively stable. Figure 6(d) shows that the downward trend of frequency multiplication is uniform, which further illustrates the stability of the laser.

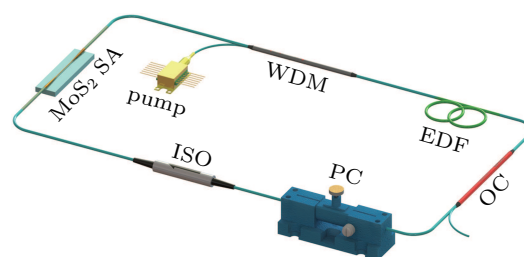


Fig. 5. (color online) Experimental illustrative diagram of Q-switching EDFL employed with MoS<sub>2</sub> SA.

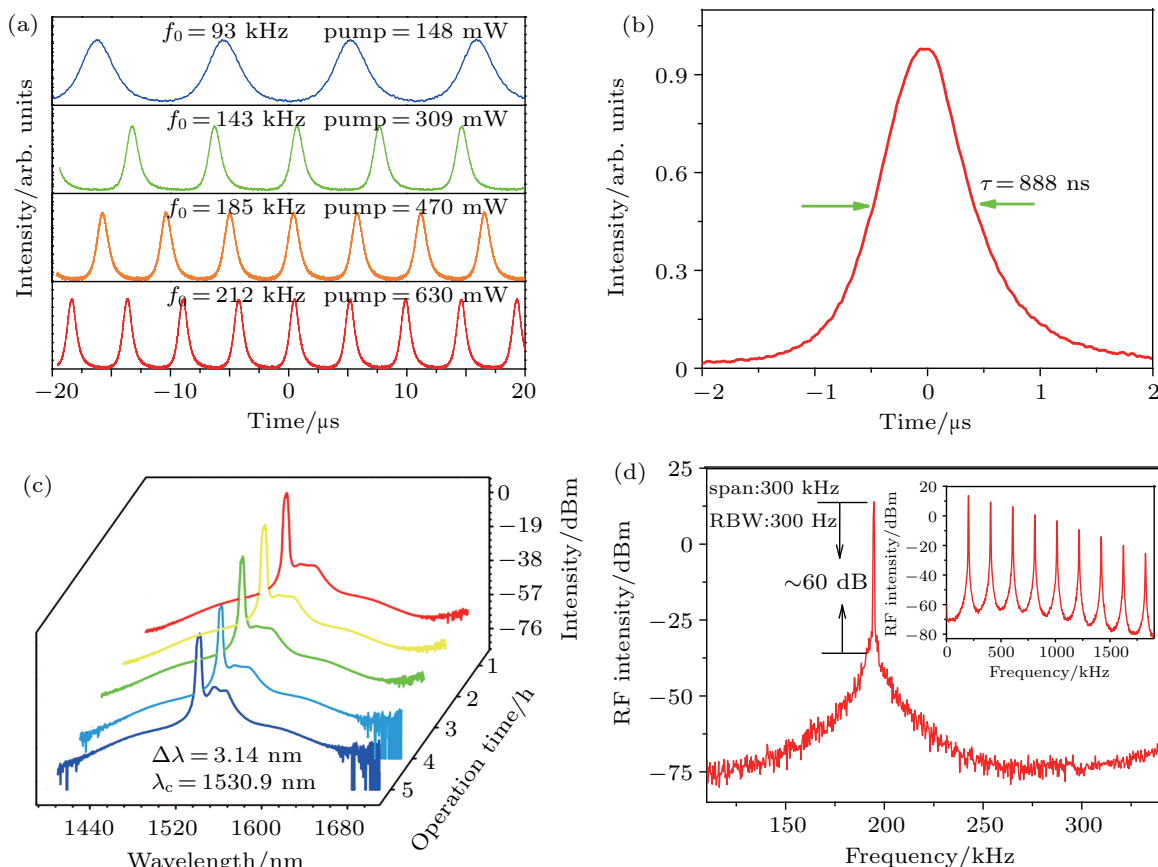


Fig. 6. (color online) Experimental data of Q-switching EDFL employed with MoS<sub>2</sub> SA, showing (a) Q-switching pulse trains at different powers, (b) single pulse waveform of Q-switching EDFL, (c) spectra at different times, and (d) RF spectrum of Q-switching EDFL.

According to the experimental monitoring data at different powers, the variation tendency of pulse duration and frequency rate with input power are shown in Fig. 7(a). In the prophase of the power growth, the pulse duration changes more sharply. However, in the later stage of power growth, the pulse duration tends to be stable. This illustrates that MoS<sub>2</sub> SA is close to saturation at high power. With the increase of power, the repetition rate is almost increased uniformly. Similarly, we record and calculate the corresponding output power and pulse energy of the Q-switched pulse train varying with pump power in Fig. 7(b). On the whole, not only output power but also pulse energy increase evenly with input power. The ultimate output power and pulse energy are obtained to be 18.8 mW and 88 nJ, respectively. The maximum damage threshold is about 19.5 mJ/cm<sup>2</sup>.

Performance comparisons of Q-switched EDFL based on different SAs are shown in Table 2. By comparison, the CVD-MoS<sub>2</sub> has certain potentials and advantages in realizing short pulse duration. Moreover, the SNR of most Q-switched EDFL is below 50 dB. The SNR of Q-switched EDFL based on CVD-MoS<sub>2</sub> increases up to 60 dB, which indicates the stability of operation. These results show that the microfiber-MoS<sub>2</sub> SA prepared by the CVD method is able to support stable Q-switching operation, which means it can serve as an impactful

nonlinear control device for Q-switching EDFL.

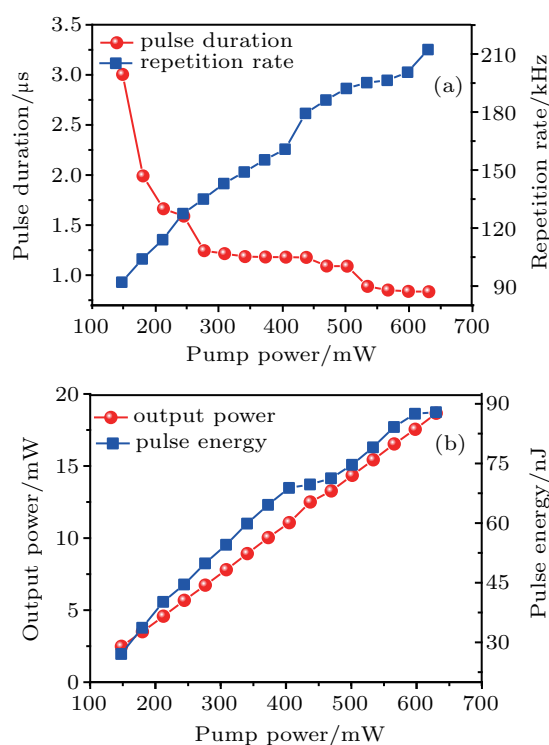


Fig. 7. (color online) (a) Variation of pulse duration and frequency rate with pump power, and (b) variation of output power and pulse energy with pump power.

Table 2. Performance comparisons of Q-switched EDFL based on different SAs.

Materials	$\alpha_s/\%$	$\tau/\mu\text{s}$	Frequency/kHz	Energy/nJ	SNR/dB	Output power/mW	Ref.
MoS <sub>2</sub>	4	3.53	72.74–86.39	74.93	51.6	6.47	[60]
WS <sub>2</sub>	4.48	0.16	91–318	54.4	40	17.3	[67]
WSe <sub>2</sub>	3.02	4.1	46.3–85.4	484.8	41.9	3.16	[43]
MoSe <sub>2</sub>	–	30.4	16.9–32.8	57.9	–	1.9	[68]
Bi <sub>2</sub> Se <sub>3</sub>	4.3	1.9	495–940	23.8	50	22.35	[69]
BP	18.55	10.32	6.983–15.78	94.3	45	1.5	[45]
MoS <sub>2</sub>	11.07	0.888	92–212	88	60	18.8	this work

## 4. Conclusions

By combining the CVD method with the PMMA assisted method, the MoS<sub>2</sub> SA based on microfiber is successfully produced. On the one hand, the films prepared by the CVD method are of good uniformity. On the other hand, the gold-plated SA based on microfiber has some advantages in preventing heat-resistant damage, and anti-oxidation. The saturation intensity and MD of MoS<sub>2</sub> SA are 1.871 MW/cm<sup>2</sup> and 11.07%, respectively. Moreover, the obtained MoS<sub>2</sub> SA is successfully applied to the Q-switching EDFL. The shortest pulse duration of laser is 888 ns, and the tunable range of frequency is 92 kHz–212 kHz. The ultimate output power and pulse energy are 18.8 mW and 88 nJ, respectively. The SNR of laser increases up to 60 dB, which illustrates the stability of the operation. These results show that the microfiber-MoS<sub>2</sub> SA prepared by the CVD method is able to support stable Q-

switching pulse output, and it can serve as an impactful nonlinear control device for Q-switching EDFL.

## References

- [1] Keller U 2003 *Nature* **424** 831
- [2] Okhotnikov O, Grudinin A and Pessa M 2004 *New J. Phys.* **6** 177
- [3] Bao Q L, Zhang H, Wang Y, Ni Z H, Yan Y L, Shen Z X, Loh K P and Tang D Y 2009 *Adv. Funct. Mater.* **19** 3077
- [4] Liu W J, Liu M L, Yin J D, Chen H, Lu W, Fang S B, Teng H, Lei M, Yan P G and Wei Z Y 2018 *Nanoscale* **10** 7971
- [5] Liu W J, Liu M L, OuYang Y Y, Hou H R, Ma G L, Lei M and Wei Z Y 2018 *Nanotechnology* **29** 174002
- [6] Zhang H, Bao Q L, Tang D Y, Zhao L M and Loh K P 2009 *Appl. Phys. Lett.* **95** 141103
- [7] Sun Z P, Hasan T, Torrisi F, Popa D, Privitera G, Wang F Q, Bonaccorso F, Basko D M and Ferrari A C 2010 *ACS Nano* **4** 803
- [8] Luo A P, Zhu P F, Liu H, Zheng X W, Zhao N, Liu M, Cui H, Luo Z C and Xu W C 2014 *Opt. Express* **22** 27019
- [9] Sotor J, Bogusławski J, Martynkien T, Mergo P, Krajewska A, Przewłoka A, Strupiński W and Sobolewski G 2017 *Opt. Lett.* **42** 1592

- [10] Luo Z Q, Liu C, Huang Y Z, Wu D D, Wu J Y, Xu H Y, Cai Z P, Lin Z Q, Sun L P and Weng J 2014 *IEEE J. Sel. Top. Quantum Electron.* **20** 0902708
- [11] Sotor J, Sobon G, Grodecki K and Abramski K M 2014 *Appl. Phys. Lett.* **104** 251112
- [12] Liu H, Zheng X W, Liu M, Zhao N, Luo A P, Luo Z C, Xu W C, Zhang H, Zhao C J and Wen S C 2014 *Opt. Express* **22** 6868
- [13] Liu W J, Pang L H, Han H N, Tian W L, Chen H, Lei M, Yan P G and Wei Z Y 2016 *Sci. Rep.* **6** 19997
- [14] Sotor J, Sobon G, Macherzynski W, Paletko P and Abramski K M 2015 *Appl. Phys. Lett.* **107** 051108
- [15] Hu G H, Albrow-Owen T, Jin X X, Ali A, Hu Y W, Howe R C T, Shehzad K, Yang Z Y, Zhu X K, Woodward R I, Wu T C, Jussila H, Wu J B, Peng P, Tan P H, Sun Z P, Kelleher E J R, Zhang M, Xu Y and Hasan T 2017 *Nat. Commun.* **8** 278
- [16] Li J F, Luo H Y, Zhai B, Lu R G, Guo Z N, Zhang H and Liu Y 2016 *Sci. Rep.* **6** 30361
- [17] Liu S C, Zhang Y N, Li L, Wang Y G, Lv R D, Wang X, Chen Z D and Wei L L 2018 *Appl. Opt.* **57** 1292
- [18] Yun L 2017 *Opt. Express* **25** 32380
- [19] Xu Y H, Wang Z T, Guo Z N, Huang H, Xiao Q L and Zhang H 2016 *Adv. Opt. Mater.* **4** 1223
- [20] Jiang X T, Liu S X, Liang W Y, Luo S J, He Z L, Ge Y Q, Wang H D, Cao R, Zhang F, Wen Q, Li J Q, Bao Q L, Fan D Y and Zhang H 2018 *Laser Photon. Rev.* **12** 1700229
- [21] Li W Y, OuYang Y Y, Ma G L, Liu M L and Liu W J 2018 *Laser Phys.* **28** 055104
- [22] Liu W J, Liu M L, Lei M, Fang S B and Wei Z Y 2018 *IEEE J. Sel. Top. Quantum Electron.* **24** 0901005
- [23] Yang C Y, Li W Y, Yu W T, Liu M L, Zhang Y J, Ma G L, Lei M and Liu W J 2018 *Nonlinear Dyn.* **92** 203
- [24] Zhang M, Howe R C T, Woodward R I, Kelleher E J R, Torrisi F, Hu G H, Popov S V, Taylor J R and Hasan T 2015 *Nano Res.* **8** 1522
- [25] Pumera M, Sofer Z and Ambrosi A 2014 *J. Mater. Chem. A* **2** 8981
- [26] Yan P G, Liu A J, Chen Y S, Chen H, Ruan S C, Guo C Y, Chen S F, Li I L, Yang H P, Hu J G and Cao G Z 2015 *Opt. Mater. Express* **5** 479
- [27] Li W Y, Ma G L, Yu W T, Zhang Y J, Liu M L, Yang C Y and Liu W J 2018 *Chin. Phys. B* **27** 030504
- [28] Liu M L, Liu W J, Yan P G, Fang S B, Teng H and Wei Z Y 2018 *Chin. Opt. Lett.* **16** 020007
- [29] Yu W T, Yang C Y, Liu M L, Zhang Y J and Liu W J 2018 *Optik* **159** 21
- [30] Huang X, Zeng Z Y and Zhang H 2013 *Chem. Soc. Rev.* **42** 1934
- [31] Wang J T, Jiang Z K, Chen H, Li J R, Yin J D, Wang J Z, He T C, Yan P G and Ruan S C 2017 *Opt. Lett.* **42** 5010
- [32] Liu W J, Pang L H, Han H N, Shen Z W, Lei M, Teng H and Wei Z Y 2016 *Photon. Res.* **4** 111
- [33] Zhang M, Hu G H, Hu G Q, Howe R C T, Chen L, Zheng Z and Hasan T 2015 *Sci. Rep.* **5** 17482
- [34] Liu W J, Zhu Y N, Liu M L, Wen B, Fang S B, Teng H, Lei M, Liu L M and Wei Z Y 2018 *Photon. Res.* **6** 220
- [35] Liu M L, Liu W J, Pang L H, Teng H, Fang S B and Wei Z Y 2018 *Opt. Commun.* **406** 72
- [36] Liu W J, Yang C Y, Liu M L, Yu W T, Zhang Y J and Lei M 2017 *Phys. Rev. E* **96** 042201
- [37] Mao D, She X Y, Du B B, Yang D X, Zhang W D, Song K, Cui X Q, Jiang B Q, Peng T and Zhao J L 2016 *Sci. Rep.* **6** 23583
- [38] Wang Q H, Kalantar-Zadeh K, Kis A, Coleman J N and Strano M S 2012 *Nat. Nanotechnol.* **7** 699
- [39] Britnell L, Ribeiro R M, Eckmann A, Jalil R, Belle B D, Mishchenko A, Kim Y J, Gorbachev R V, Georgiou T, Morozov S V, Grigorenko A N, Geim A K, Casiraghi C, Castro Neto A H and Novoselov K S 2013 *Science* **340** 1311
- [40] Du J, Wang Q K, Jiang G B, Xu C W, Zhao C J, Xiang Y J, Chen Y, Wen S C and Zhang H 2015 *Sci. Rep.* **4** 6346
- [41] Zhang H, Lu S B, Zheng J, Du J, Wen S C, Tang D Y and Loh K P 2014 *Opt. Express* **22** 7249
- [42] Wang S X, Yu H H, Zhang H J, Wang A Z, Zhao M W, Chen Y X, Mei L M and Wang J Y 2014 *Adv. Mater.* **26** 3538
- [43] Chen B H, Zhang X Y, Wu K, Wang H, Wang J and Chen J P 2015 *Opt. Express* **23** 26723
- [44] Wang K P, Wang Jun, Fan J T, Lotya M, O'Neill A, Fox D, Feng Y Y, Zhang X Y, Jiang B X, Zhao Q Z, Zhang H Z, Coleman J N, Zhang L and Blau W J 2013 *ACS Nano* **7** 9260
- [45] Chen Y, Jiang G B, Chen S Q, Guo Z N, Yu X F, Zhao C J, Zhang H, Bao Q L, Wen S C, Tang D Y and Fan D Y 2015 *Opt. Express* **23** 12823
- [46] Aiub E J, Steinberg D, de Souza E A T and Saito L A M 2017 *Opt. Express* **25** 10546
- [47] Wu K, Zhang X Y, Wang J, Li X and Chen J P 2015 *Opt. Express* **23** 11453
- [48] Koo J, Park J, Lee J, Jhon Y M and Lee J H 2016 *Opt. Express* **24** 10575
- [49] Guo B, Yao Y, Yan P G, Xu K, Liu J J, Wang S G and Li Yuan 2016 *IEEE Photon. Technol. Lett.* **28** 323
- [50] Liu W J, Pang L H, Han H N, Liu M L, Lei M, Fang S B, Teng H and Wei Z Y 2017 *Opt. Express* **25** 2950
- [51] Yan P G, Chen H, Yin J D, Xu Z H, Li J R, Jiang Z K, Zhang W F, Wang J Z, Li I L, Sun Z and Ruan S C 2017 *Nanoscale* **9** 1871
- [52] Zhao L M, Tang D Y, Zhang H, Wu X, Bao Q L and Loh K P 2010 *Opt. Lett.* **35** 3622
- [53] Chen H, Chen Y S, Yin J D, Zhang X J, Guo T and Yan P G 2016 *Opt. Express* **24** 16287
- [54] Yan P G, Lin R Y, Ruan S C, Liu A J and Chen H 2015 *Opt. Express* **23** 154
- [55] Wu K, Chen B H, Zhang X Y, Zhang S F, Guo C S, Li C, Xiao P S, Wang J, Zhou L J, Zou W W and Chen J P 2018 *Opt. Commun.* **406** 214
- [56] Li H, Zhang Q, Yap C C R, Tay B K, Edwin T H T, Olivier A and Baillargeat D 2012 *Adv. Funct. Mater.* **22** 1385
- [57] Zhao Y Y, Luo X, Li H, Zhang J, Araujo P T, Gan C K, Wu J, Zhang H, Quek S Y and Dresselhaus M S 2013 *Nano Lett.* **13** 1007
- [58] Lee C, Yan H, Brus L E, Heinz T F, Hone J and Ryu S 2010 *ACS Nano* **4** 2695
- [59] Lou F, Zhao R W, He J L, Jia Z T, Su Xi C, Wang Z W, Hou J and Zhang B T 2015 *Photon. Res.* **3** A25
- [60] Luo Z C, Wang F Z, Liu H, Liu M, Tang R, Luo A P and Xu W C 2016 *Opt. Eng.* **55** 081308
- [61] Huang Y Z, Luo Z Q, Li Y Y, Zhong M, Xu B, Che K J, Xu H Y, Cai Z P, Peng J and Weng J 2014 *Opt. Express* **22** 25258
- [62] Woodward R I, Kelleher E J R, Howe R C T, Hu G, Torrisi F, Hasan T, Popov S V and Taylor J R 2014 *Opt. Express* **22** 31113
- [63] Luo Z Q, Huang Y Z, Zhong M, Li Y Y, Wu J Y, Xu B, Xu H Y, Cai Z P, Peng J and Weng J 2014 *J. Lightwave Technol.* **32** 4077
- [64] Ren J, Wang S X, Cheng Z C, Yu H H, Zhang H J, Chen Y X, Mei L M and Wang P 2015 *Opt. Express* **23** 5607
- [65] Xia H D, Li H P, Lan C Y, Li C, Zhang X X, Zhang S J and Liu Y 2014 *Opt. Express* **22** 17341
- [66] Xia H D, Li H P, Lan C Y, Li C, Du J B, Zhang S J and Liu Y 2015 *Photon. Res.* **3** A92
- [67] Chen H, Li L, Ruan S C, Guo T and Yan P G 2016 *Opt. Eng.* **55** 081318
- [68] Ahmad H, Suthaskumar M, Tiu Z C, Zarei A and Harun S W 2016 *Opt. Laser Technol.* **79** 20
- [69] Yu Z H, Song Y R, Tian J R, Dou Z Y, Guoyu H Y, Li K X, Li H W and Zhang X P 2014 *Opt. Express* **22** 11508